Middle East Journal of Applied Sciences
Volume: 16 | Issue: 02| April – June | 2026

EISSN: 2706 -7947 ISSN: 2077- 4613
DOI: 10.36632/mejas/2026.16.2.8
Journal homepage: www.curresweb.com
Pages: 110-123

Radioactivity and Geotechnical Studies of New Mansoura City, Egypt

Osama M. Draz

Nuclear Materials Authority, P. O. Box 530, El-Maadi, Cairo, Egypt.

Received: 10 March 2026 **Accepted:** 20 May 2026 **Published:** 15 June 2026

ABSTRACT

New Mansoura is a part of eastern north of Nile Delta which located on the coast of Mediterranean Sea, 50 soil samples were taken from 50 boreholes 10 m deep. Interpreting the obtained results divided soil profile in two main types loose to medium dense, poorly graded, fine to medium-grained sand followed by high plasticity silt with sand. The main geotechnical hazards in New Mansoura is soil aggression from intrusion of sea water. Radioactively New Mansoura is safe, naturally occurring radionuclides ^{238}U, ^{232}Th, ^{226}Ra and ^{40}K in sediments were measured using Sodium Iodide Detector. The concentrations of ^{238}U ranging from ULD to 37.05 with average 20.501 Bq Kg^{-1}, ^{232}Th ranging from 8.12 to 28.42 with average 18.216 Bq $Kg,^{-1}$ ^{226}Ra ranging from 11.10 to 77.70 with average 36.853 Bq $Kg,^{-1}$ while ^{40}K ranging from 435.07 to 544.62 with average 469.85 Bq $Kg,^{-1}$ The activity concentrations of ^{238}U, ^{232}Th, ^{226}Ra are within the acceptable limit as recommended by the International Atomic Energy Agency (IAEA, 1989) except the concentration of ^{40} K is higher than the acceptable limit.

Keywords: New Mansoura, Nile Delta, soil samples, medium dense, poorly graded, radionuclides, International Atomic Energy Agency

Introduction

New Mansoura is one of new cities in many parts of Egypt. It is located in the northeastern part of Nile delta. It is bounded by latitudes 31° 33' 15" N and 31° 25' 15" N, longitudes 31° 32' 45" E and 31° 17' 45" E (Fig. 1). The current work is separated into two components. The first one focused on geotechnical qualities, including physical and mechanical properties of the foundation bed spread in the study region. The second one is radioactivity measurements and the different sources of natural radiation and their ecological risk assessment in New Mansoura. The city is completely covered by marine sediments and black sand. Black sand is distributed along the northern coastal plain from Abu-Qir to Rafah.

Geologic setting and stratigraphy of the study area

The study area is a semi-flat elevated with average of 0 – 2 m above sea level, lies on the coast of Mediterranean Sea, which completely covered by marine sediments and black sand. In the Late Pliocene, a paleo-Nile began to move over a marine embayment and evolved particularly throughout the Pleistocene as a result of significant sea-level fluctuations linked to glacial periods. A significant amount of mud and sand was carried and scattered around the Eastern Mediterranean during low sea-level. The study area is characterized by very gentle topography.

The different litho-stratigraphic units that are exposed on the surface and encountered in the sub-surface as shown in (Figs. 2 & 3). Geologically the sediments of the study area are related to late quaternary and divided into:

Corresponding Author: Osama M. Draz, Nuclear Materials Authority, P. O. Box 530, El-Maadi, Cairo, Egypt.

1. Near-shore sand

Near-shore sand deposits are composed of fine sand, rich in heavy minerals and poor in quartz with thickness of 4 to 58 m.

2. Coastal dune sand

It is very fine to fine sand, which has a low percent of a heavy mineral and a high percent of quartz. It has a thickness of about 4 and 12 m.

3. The mud of the Nile Delta

Intercalated mud, silt, and sand, which have a light olive grey to a dark grey color.

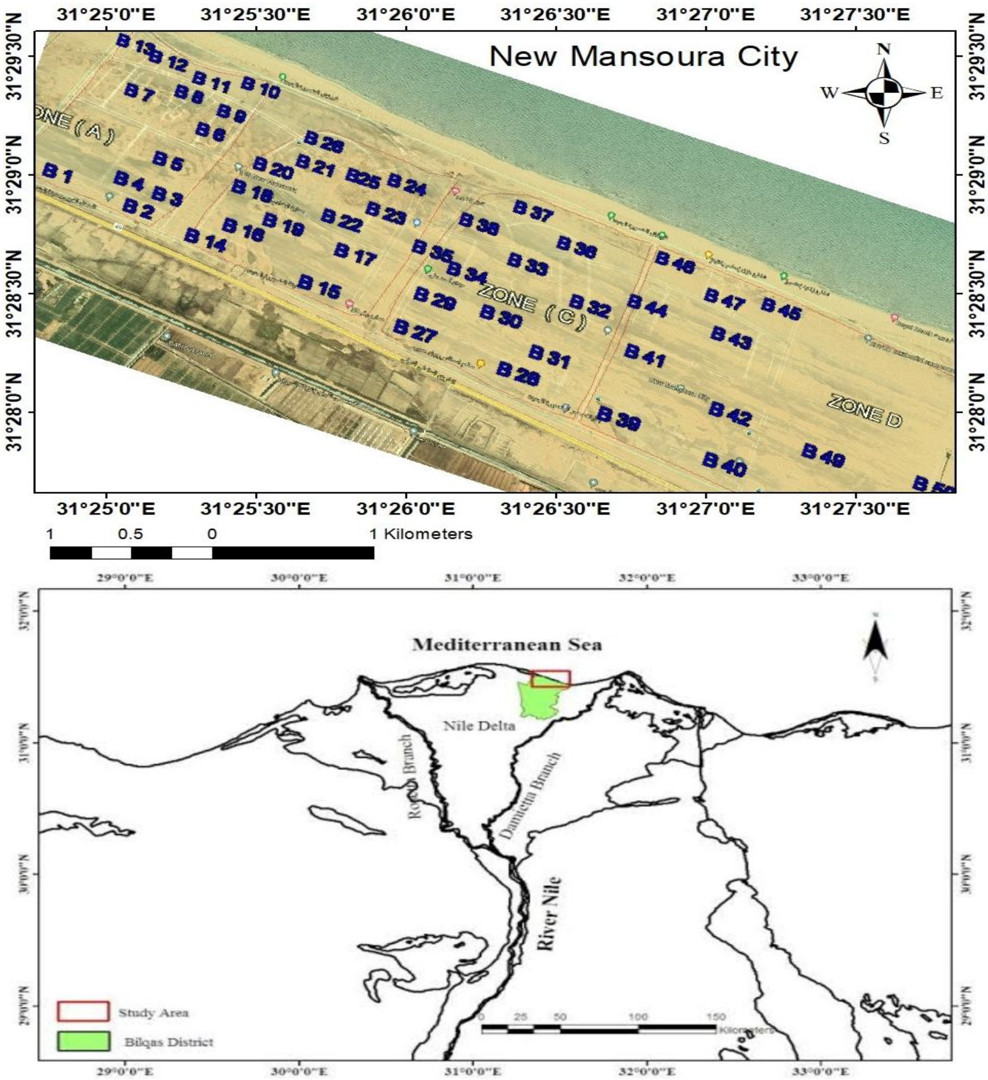

Fig. 1: Location map of the study area and samples

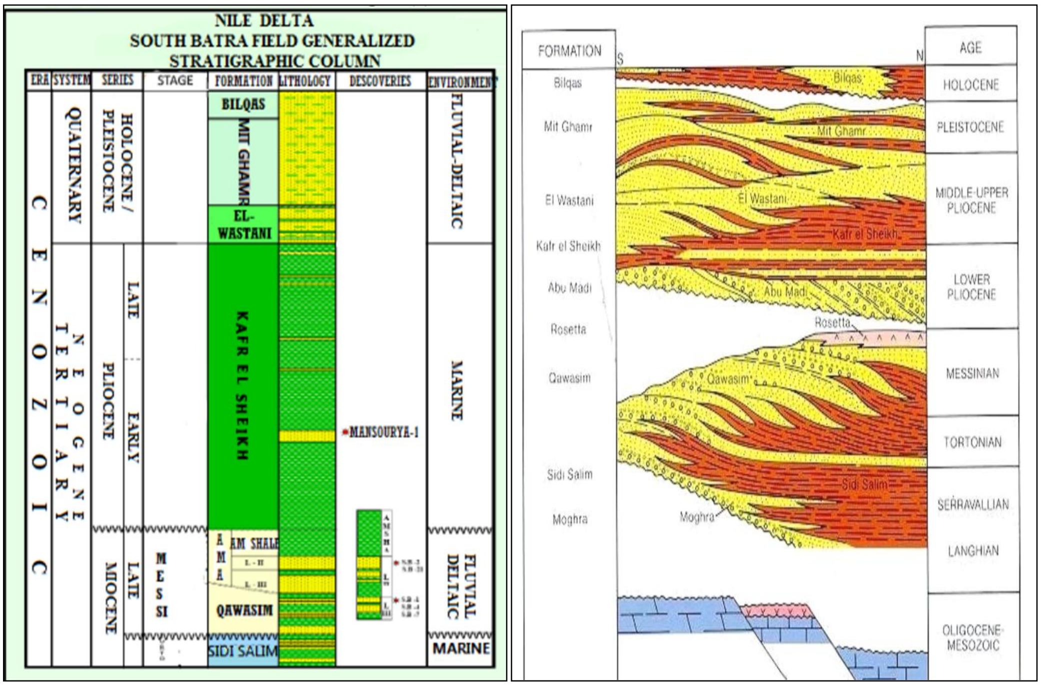

Fig. 2: Composite Stratigraphic Section of the Study Area **(After Schlumberger, 1984).**

Sampling and analytical techniques

Fifty soil samples were taken from 50 boreholes 10 m deep (Fig. 1), which taken from standard penetration test sampler at every one meter (1, 2, 3, 4, etc..) and testing samples selected every change in soil texture to detect the geotechnical parameters through laboratory tests, which used to geotechnical hazard calculations. Physical and mechanical tests include moisture content (ASTM D22216-19), sieve analysis (ASTM D6913M-17), specific gravity (ASTM D854-14), relative density (ASTM D4254-16), shear box (ASTM D3080-11), permeability (ASTM D2434-19); chemical test (BS 1377), including total dissolved salt (TDS), pH, chloride content (Cl^-), sulphate content (So_3^{++}) and $CaCo_3$ content (ASTM D3042-17).

The collected samples were prepared for measuring their contents of ^{238}U, ^{226}Ra, ^{232}Th and ^{40}K and analyzed at Sodium Iodide Detector laboratory, Authority of Nuclear Materials, Egypt. Uranium is estimated both as eU and Ra (eU) and thorium as eTh. The values of eU represent the concentration of U using ^{234}Th energy peak (93 keV) and measure the first daughter isotope in the ^{238}U decay series with very low possible loss. Radium is measured at the ^{214}Pb energy peak (352 keV) which is considered as a measure for concentration of the U only in case of the secular equilibrium state between ^{238}U and all its daughter isotopes. Thorium is measured from ^{212}Pb energy peak (238 keV).

Geotechnical Laboratory Results

Soil profile of New Mansoura City can be classified into loose dense, poorly graded fine to medium grained sand with thickness 6 m followed by poorly graded, brown to black sand plasticity silt, with thickness 4 m. The results of geotechnical parameters of New Mansoura City soil layers given in Tables (1 & 2).

Boreholes were obtained from a mechanical rig (a rotary drilling rig) at depths from zero to 10 meters (from the surface of the earth), as shown in Figure 4.

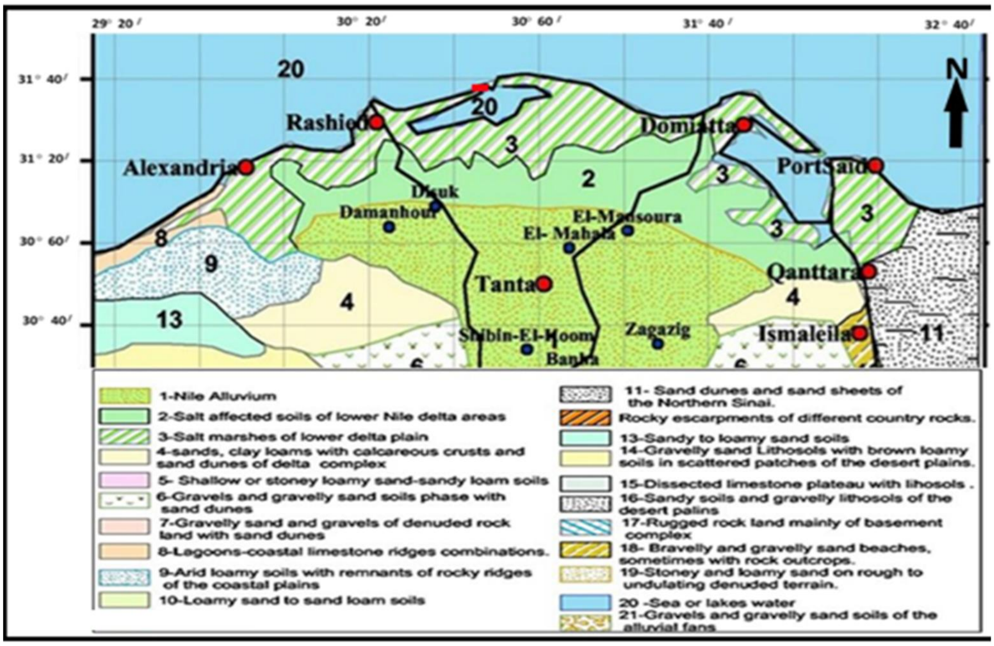

Fig. 3: Geological Map of the Study Area **(After CONCO-Coral, 1987).**

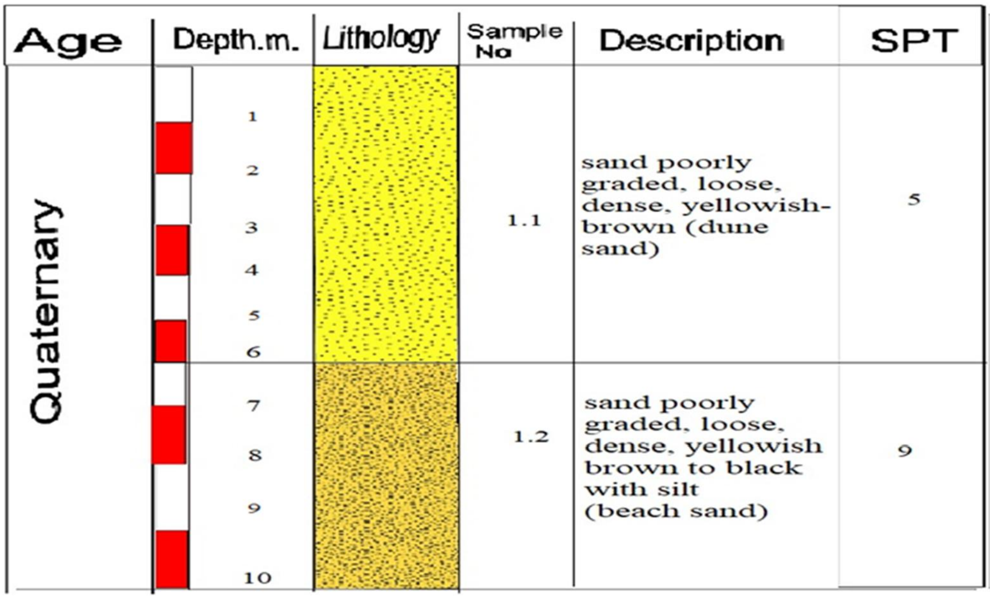

Fig. (4): Bore hole obtained from mechanical rig

SPT value Correction

Youd *et al*., 2003 produced a standard curve for fine content in sand as an effective parameter in CRR calculation and gave it the name, clean-sand base curve. This curve is fitted to represent low (N1) 60 < 30 and intercept at fine percent 5% as in (Figure 5). The curve was reproduced to Seed's and Idriss (1971) correction equation for fine content correction SPT value; (N1) 60 CS to represent clean sand status:

$$(N_1)_{60CS} = \alpha + \beta(N_1)_{60} \qquad \rightarrow \qquad (1)$$

α and β = constant proportions with fine content.

There are more elements, beyond fines content, that determine SPT value. Equation (2) incorporates these corrections.

$$(N_1)_{60} = N_m C_N C_E C_B C_R C_S \qquad \rightarrow \qquad (2)$$

Where (N1) 60 is the SPT number at an overburden stress 1 atmosphere and 60% from the efficiency of the hammer. N_m is measured as the standard penetration value; C_N, C_E, C_B, C_R, and C_S are factors in the correction of overburden pressure, hammer energy, bore-hole diameter, rod length, and spoon liner respectively. CRR calculated by the (eq. 3):

$$CRR_{7.5} = \frac{1}{34-(N_1)_{60}} + \frac{(N_1)_{60}}{135} + \frac{50}{10[(N_1)_{60}+45]^2} - \frac{1}{2\ 00} \quad \rightarrow \quad (3)$$

When (N1) 60 > 30, sandy and gravelly soils become dense and non-liquefaction soil, Seed *et al*. (1985) noted that the increasing fine fraction in sand soil leads to an increase in CRR.

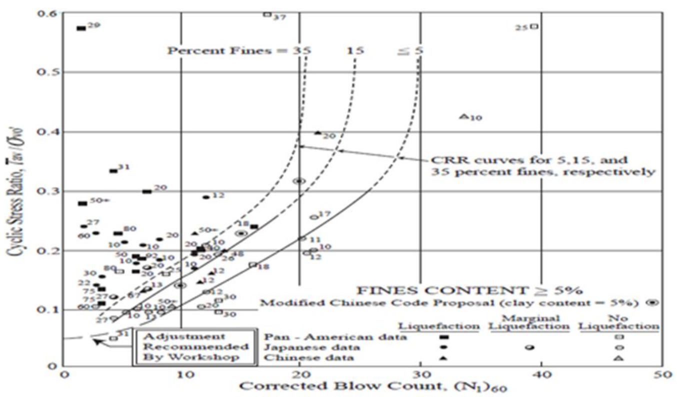

Fig. 5: Simplified base curves recommended for calculation of CRR from SPT data, along with empirical liquefaction data, (after Seed, *et al*., 1985 and Robertson and Fear, 1997).

Table 1: Results of geotechnical properties of New Mansoura City

Item	Unit	Minimum	Maximum	Average.
Water content	%	2.9	21.8	12.3
Specific gravity	--	2.331	2.715	2.512
Unit weight	kN/m^2	15.93	19.11	17.82
Relative density	%	21.94	57.62	38.46
CaCo3	%	1.93	9.84	4.42
Cl	PPM	10934	11883	11164
SO_3^{--}	PPM	2112	8002	5834
Conductivity	(Ω/m)	207	377	281
Cohesion	Kn/m^2	4	21	12
Fraction Angel	o	27o	33o	30o
Void Ratio	%	55.7	87.1	78.3
Collapsibility Index	--	1.402	1.653	1.514

Collapsible probability of sand soil at New Mansoura City according to an equation of (Das, 2011); Eq. (4) gives a range between 1.402 and 1.653 with average 1.514, the results revealed that the New Mansoura City sand soils can classified as non-collapsible soils.

$$\gamma_d \leq \frac{G_s\gamma_w}{1+e_o} = \frac{G_s\gamma_w}{1+(LL\%\ xG_s)}\ KN \quad \rightarrow \quad (4)$$

Where e_o Void ratio, G_s specific gravity, LL liquid limit, γ_d dry density and γ_w water specific gravity

Table 2: Results of geotechnical properties of New Mansoura Silt

Parameters Unit	Liquid limit (%)	Plastic limit (%)	Plasticity index (%)	Water content (%)	Consistency index (%)	Swelling pressure (kPa)
Maximum	78.6	41.3	42.9	25.4	1.6	131.2
Minimum	60.3	30.5	25.8	18.5	1.1	58.3
Average	70.5	36.4	35.1	21.1	1.5	105.3

Swelling potential values of New Mansoura according to equation (5) range between 58.3 kPa and 131.2 kPa with average 105.3 kPa, according to Gelany *et al*. (2019) classification the New Mansoura City silt soils are classified as low swelling potential soil.

$$\mathbf{P}s = \mathbf{(3.71 * LL - 125)}/CI \quad \mathbf{kPa} \qquad \rightarrow (5)$$

Where Ps Swelling pressure, CI consistency index and LL liquid limit. Relative density of sand layer was ranging from 21.94 %, which classified as loose sand to 57.62 %, which classified as medium dense sand with average 38.46 % classified as loose sand (Das, 2010).

Results of sieve analysis and grain size distribution indicate that the upper ten meters of New Mansoura has high liquefaction possibility according to (Ministry of Transportation Japanese code, 1999), because it is poorly graded fine sand with low non-plastic fine content > 10 %. The pore water pressure built up faster than drainage under earthquake load leading to lose of effective strength of soil and liquefaction.

Radioactivity

Radioactivity pollution is coming from natural and artificial sources. Natural sources of radioactivity are about 80% of the environmental radiation (UNSCEAR., 1988). Man-made radionuclides sources are nuclear and non-nuclear industries. The artificial radioactivity is coming from several sources such as phosphate fertilizers manufacture, agriculture application and coal combustion cement activities which are non-nuclear industries which distributed in increasing amounts of radioactive matter resulted in radio-ecological pollution (UNSCEAR, 1988). The interaction between the radiation and human body that resulted from the external sources outside the human body in its surrounding environment or from internal contamination of the body by radioactive substances which may cause clinical symptoms in the human body (UNSCEAR, 2000). Gamma radiation emission sources are the naturally occurring radioisotopes such as radionuclides from ^{232}Th, ^{238}U series and ^{40}K and their decay products which are also known as terrestrial background radiation. They represent the main external source of irradiation to the human body (Harb, 2008). The increased levels of terrestrial gamma radiation are dependent on the presence of radioisotopes in the soils. Many studies assessed the terrestrial gamma-ray dose rate in the air (Faheem *et al*.; 2008, Lee *et al*.; 2009, Taskin *et al*.; 2009, El-Taher *et al*., 2010) in which around 85% of the annual total radiation dose is originated from natural radionuclides of both terrestrial and cosmogenic origin (Belivermis *et al*., 2010; NCRP, 1994; UNSCEAR, 2000). In this study we try to identify the natural radiation and their ecological risk assessment in New Mansoura

Table (3) shows the distribution concentrations of natural radionuclide, ^{238} U, ^{232} Th, ^{226} Ra, and ^{40} K of the studied samples, while the average specific activity concentrations of ^{238} U (^{226} Ra) series, ^{232} Th series, and ^{40} K, expressed in Bq / kg dry weight together with the ^{238} U (^{226} Ra) / ^{232} Th ratio and the radium equivalent for each sample were calculated while fig. 6 shows concentrations of the natural radionuclide, ^{238}U, ^{232}Th, ^{226}Ra, and ^{40}K of the study area.

The activity concentrations of the studied samples in Bq / Kg were determined from the photo peaks of the gamma-ray spectra corresponding to ^{238} U, ^{232} Th, and ^{40} K. The values of eU and eTh in ppm as well as K in percent were converted to activity concentrations (Bq / Kg), using the conversion factors given by IAEA, (1989).

Table 3: The distribution concentrations of natural radionuclide, ^{238}U, ^{232}Th, ^{226}Ra, and ^{40}K of the studied samples.

Sample No.	^{238}U Concentration		^{232}Th Concentration		^{226}Ra Concentration		^{40}K Concentration	
	ppm	Bq/Kg	ppm	Bq/Kg	Ppm	Bq/Kg	%	Bq/Kg
1	1	12.35	3	12.18	3	33.3	1.44	450.72
2	2	24.7	3	12.18	6	66.6	1.54	482.02
3	3	37.05	4	16.24	7	77.7	1.74	544.62
4	ULD	ULD	3	12.18	3	33.3	1.55	485.15
5	1	12.35	3	12.18	2	22.2	1.55	485.15
6	1	12.35	3	12.18	5	55.5	1.46	448.13
7	2	24.7	5	20.3	1	11.1	1.44	444.46
8	1	12.35	3	12.18	4	44.4	1.65	513.48
9	2	24.7	3	12.18	2	22.2	1.56	491.12
10	2	24.7	5	20.3	3	33.3	1.41	433.46
11	3	37.05	7	28.42	5	55.5	1.50	472.63
12	ULD	ULD	3	12.18	1	11.1	1.48	453.10
13	3	37.05	5	20.3	4	44.4	1.48	463.24
14	1	12.35	6	24.36	1	11.1	1.61	503.93
15	1	12.35	3	12.18	7	77.7	1.51	472.63
16	ULD	ULD	3	12.18	1	11.1	1.46	456.98
17	3	37.05	2	8.12	2	22.2	1.53	478.89
18	2	24.7	1	4.06	7	77.7	1.55	485.15
19	ULD	ULD	3	12.18	2	22.2	1.49	466.37
20	2	24.7	5	20.3	4	44.4	1.39	435.07
21	1	12.35	1	4.06	3	33.3	1.47	460.11
22	3	37.05	3	12.18	2	22.2	1.66	519.58
23	1	12.35	2	8.12	5	55.5	1.70	532.1
24	2	24.7	7	28.42	2	22.2	1.57	493.25
25	1	12.35	5	20.3	3	33.3	1.50	472.63
26	2	24.7	5	20.3	5	55.5	1.46	448.13
27	2	24.7	2	8.12	1	11.1	1.55	485.15
28	3	37.05	1	4.06	4	44.4	1.48	453.10
29	1	12.35	4	16.24	1	44.4	1.61	504.87
30	1	12.35	3	12.18	7	77.7	1.59	497.7
31	1	12.35	5	20.3	1	11.1	1.40	439.12
32	3	37.05	6	24.36	2	22.2	1.63	507.06
33	2	24.7	6	24.36	7	77.7	1.57	493.21
34	3	37.05	5	20.3	2	22.2	1.50	472.63
35	2	24.7	7	28.42	2	22.2	1.47	460.11
36	2	24.7	5	20.3	5	55.5	1.46	448.13
37	1	12.35	3	12.18	2	22.2	1.49	466.37
38	3	37.05	3	12.18	2	22.2	1.66	519.58
39	1	12.35	2	8.12	5	55.5	1.70	532.1
40	1	12.35	4	16.24	1	44.4	1.61	504.87
41	1	12.35	5	20.3	1	11.1	1.40	439.12
42	3	37.05	6	24.36	2	22.2	1.63	507.06
43	1	12.35	2	8.12	3	33.3	1.55	485.15
44	3	37.05	7	28.42	5	55.5	1.50	472.63
45	ULD	ULD	3	12.18	1	11.1	1.48	453.10
46	3	37.05	5	20.3	4	44.4	1.48	463.24
47	1	12.35	6	24.36	1	11.1	1.61	503.93
48	1	12.35	3	12.18	7	77.7	1.51	472.63
49	3	37.05	4	16.24	7	77.7	1.74	544.62
50	1	12.35	5	20.3	3	33.3	1.50	472.63
Min.	ULD	ULD	2	8.12	1	11.1	1.39	435.07
Max.	3	37.05	7	28.42	7	77.7	1.74	544.62
Average	**1.66**	**20.501**	**3.96**	**18.216**	**3.32**	**36.853**	**1.504**	**469.85**

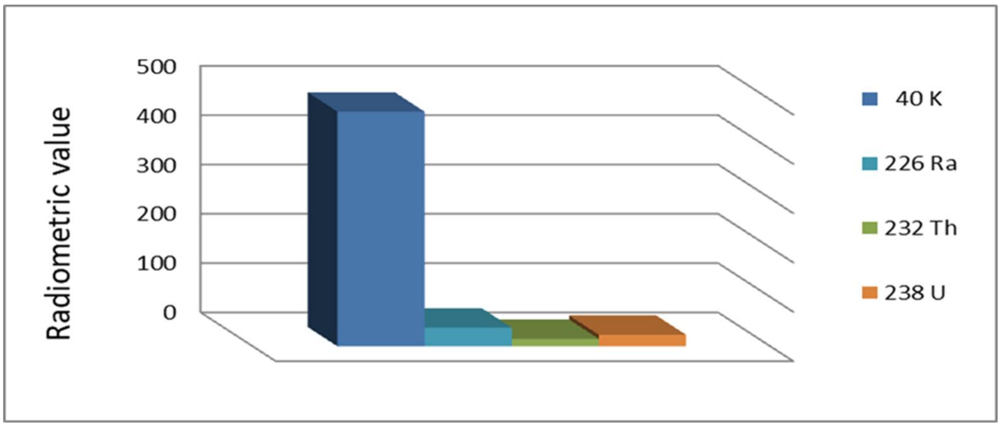

Fig. 6: The chart shows concentrations of the natural radionuclide, 238U 232Th, 226Ra, and 40K of the study area.

The activity concentration of a sample 1 ppm by weight of ^{238} U is 12.35 Bq / Kg, 1 ppm of ^{232} Th is 4.06 Bq / Kg, 1 ppm of ^{226} Ra is 11.1 Bq / Kg and 1 ppm of ^{40} K is 313 Bq/Kg.
The activity concentrations of all samples are within the acceptable limit which is 370 Bq / Kg-1 as recommended by the International Atomic Energy Agency (IAEA, 1989) except the concentration of ^{40} K is higher than the acceptable limit.

Radium equivalent activity (Ra_{eq})

Radiation hazards were measured by the radium equivalent activity (Ra_{eq}) in which ^{238}U series has been replaced by the decay product ^{226}Ra. The radium equivalent activity is an index that represents the specific activities of ^{226}Ra, ^{232}Th and ^{40}K by a single quantity. Radium equivalent activity (Raeq), is calculated by equation (6) of Beretka and Mathew (1985).

$$\mathbf{Ra_{eq} = A_{Ra} + 1.43A_{Th} + 0.077A_k} \qquad \rightarrow \qquad (6)$$

Where, A_{Ra}, A_{Th} and A_K are referred to as the values of the activity's concentrations of ^{226}Ra, ^{232}Th and ^{40}K (Bq kg–1), respectively. The Ra_{eq} values in the studied area vary from 60.4 to 344.5 Bq kg–1 with an average of 191.3 Bq kg–1 (Table 4) which is below the accepted value of Raeq (370 Bq kg–1) approved by UNSCEAR (2000).

Table 4: Shows Result of radioactive doses and external hazard at the study area

Parameter / Unit	Radium Equivalent (Ra_{eq}) Bqkg^{-}1			Effective dose rate (Deff) index (µSv y-1)			External hazard(H_{ex}) (Bqkg^{-1})		
Depth (m)	Min.	Max.	Avg.	Min.	Max.	Avg.	Min.	Max.	Avg.
1	60.4	344.5	191.3	26.1	111.3	66.4	0.15	0.98	0.46
2	41.2	251.4	133.9	28.4	105.9	65.1	0.17	0.71	0.39

External Hazard Index H_{ex}

According to, ICRP 60 (1990), the external hazard index is used as a datum against which one can know whether particular levels exceed the external radiation permissible dose equivalent limit to the population of 1.0 mSvy^{-1}. External and internal hazard indexes are hazardous to the respiratory organs

EISSN: 2706 -7947 ISSN: 2077- 4613 *DOI: 10.36632/mejas/2026.16.2.8*

(Shuaibu *et al.*, 2017). The external hazard index (H_{ex}) can be computed by equation 7 (Oktay *et al.*, 2011)

$$\mathbf{H_{ex} = (A_{Ra}/370 + A_{Th}/259 + A_K/4810) \leq 1 \quad \rightarrow \quad (7)}$$

whereas A_{Ra}, A_{Th} and A_K are the same as in the equation 6.
The results of external hazard index of the analyzed samples are between 0.15 and 0.98 Bq kg^{-1} with an average of 0.46 Bq kg^{-1}. The results did not exceed the permissible limit ≤1.

Effective Dose Rate (D_{eff})

To estimate the annual effective dose rate, the conversion coefficient from absorbed dose in the air to effective dose (0.7 µSvGy^{-1}) and outdoor occupancy factor (0.2). The effective dose rate in unit µSvy^{-1} was calculated by eq. 8:

$$\mathbf{D_{eff} = D \times 8760h \times 0.2 \times 0.7\ \mu Svy^{-1} \times 10^{-3}\ (\mu Svyr^{-1}) \quad \rightarrow (8)}$$

For the soil samples of the study area, the values of the annual effective dose range from 26.1 µSvy^{-1} to 111.3 µSvy^{-1} with an average 66.4 µSvy^{-1} of the soil samples. These values are acceptable for the worldwide levels which is approximately 70 µSvy-1

Annual gonadal dose equivalent (AGDE)

Annual gonadal dose equivalent (AGDE) is a genetic significance of the dose equivalent received each year by the reproductive organs (gonads) of the exposed population to natural radioactivity (Shousha *et al.*, 2019). The AGDE is calculated from the specific activities of ^{226}Ra, ^{232}Th and ^{40}K in the samples by using equation 9 (Mamont Ciesla *et al.*, 1982):

$$\mathbf{AGDE\ (\mu Sv\ y\text{-}1) = 3.09\ CR_a + 4.18\ C_{Th} + 0.314\ C_K \quad \rightarrow \quad (9)}$$

The maximum value of AGDE in the study area is 545.15 µSv y^{-1} whereas, the minimum value is 149.30 µSv y^{-1} with an average 244.11 µSv y^{-1}. The highest values exceeded the permissible limit (300 µSv y-1, UNSCEAR, 2000) (Fig.7).

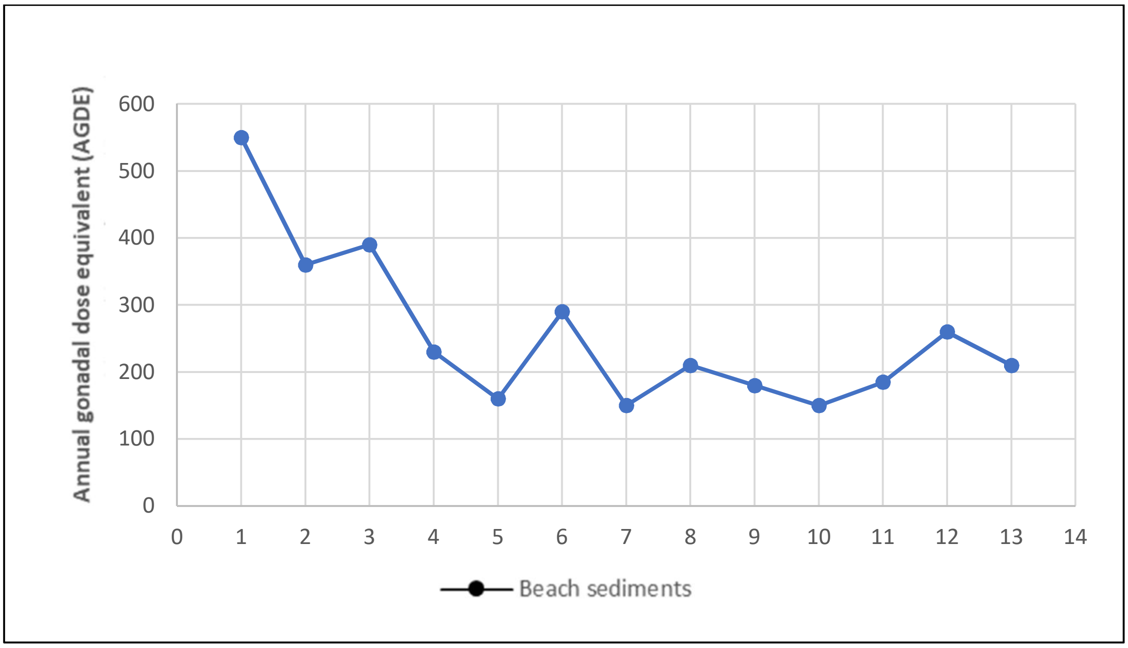

Fig. 7: The AGDE values of the study area.

Middle East J. Appl. Sci., 16(2): 110-123, 2026
EISSN: 2706 -7947 ISSN: 2077- 4613 *DOI: 10.36632/mejas/2026.16.2.8*

Activity utilization indexes (AUI)

The activity utilization index is a useful index to illustrate the indoor effect of the sediments in case of using it in building materials. This index is calculated using the following formula (Orgun *et al.*, 2007):

$$\mathbf{AUI= (C_{Ra} /33Bq/Kg)\mathit{f}_u + (C_{Th}/45Bq/Kg)\mathit{f}_{Th} + (C_K /420Bq/Kg)\mathit{f}_k} \quad \rightarrow \quad \mathbf{(8)}$$

where CR_a, C_{Th} and C_k are the activity concentrations of ^{238}U, ^{232}Th and ^{40}K in Bq/Kg respectively, f_u (0.462), f_{Th} (0.604) and f_k (0.041) are the fractional contributions to the total dose rate in air due to gamma radiation from the actual concentrations of these radionuclides.
The activity utilization index is ranged from 0.520 to 0.1329 (Fig.8). The obtained AUI value are below the permissible limit (≤ 2).

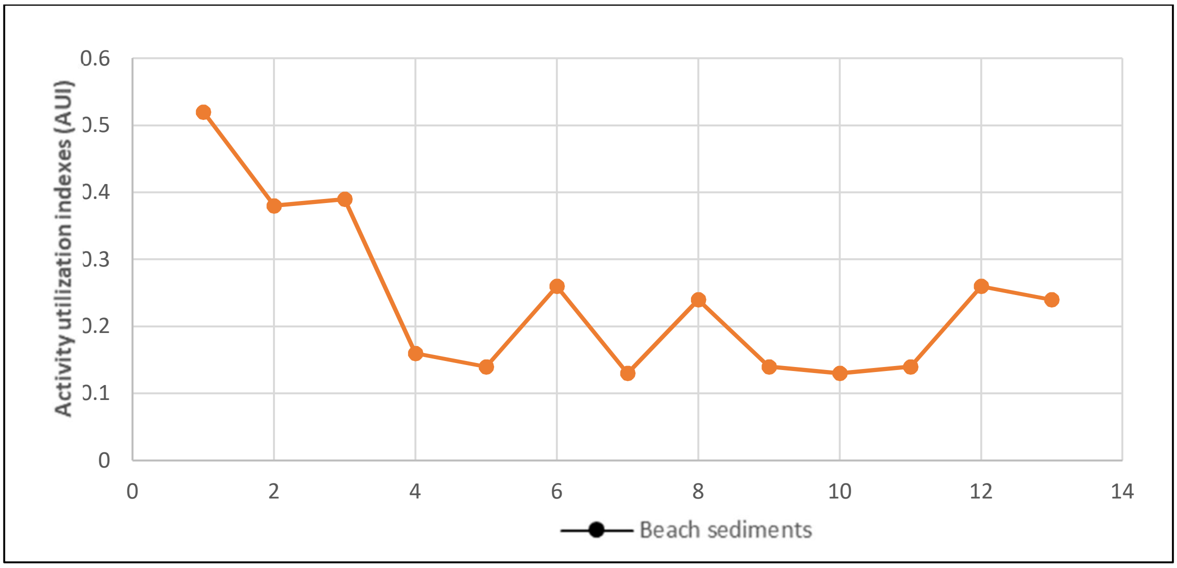

Fig. 8: The calculated AUI values of the study area.

Discussion

Comparing the obtained results in the study area with other deposits along the Mediterranean coast (Table 5) indicate that the mean activity concentrations of ^{238}U, ^{232}Th, ^{226}Ra, and ^{40}K are greater than the industrial area of port Said (Attia *et al.*, 2015), Port Said beach (Aziz *et al.*, 2020) El-Arish (Seddeek *et al.*, 2005) and Nile Delta (Ibrahim *et al.*, 1993) and much lower than their corresponding means at Baltim and Rosetta (Hilal and Borai; 2018, El-Bahi *et al.*, 2005)

A comparison of the radioactivity of the sand of the study area with those in other worldwide beach sediments is presented in table (6). The average activity concentrations of ^{232}Th and ^{226}Ra in beach sand deposits in the study area are relatively lower than the average worldwide activity concentrations in similar deposits in Iraq, Iran, Malaysia but slightly higher than that of Hungary.

Values of study area are less than the unity recommended by the International Atomic Energy Agency (IAEA, 1989) except the concentration of ^{40} K is higher than the acceptable limit, the corresponding gamma radiation hazard indices were below the acceptable limits and there is no radioactive hazard for human activities in the study area so the study area is safe.

New Mansoura soil not have collapsibility or swelling potential hazard. Liquefaction mitigation should be using soil improvement as stone column, which is suitable for New Mansoura case. New Mansoura soil can achieve the principle of sustainability; for roads using filter material and increase of roads levels and for foundation chemical resistance should be using sulphate resistant cement and concrete additives as silica fume or meta-kaoline and using bitumen isolation. For heavy and argent building using piling foundations.

Table 5: Comparison between the mean natural activity concentration of radionuclide in beach sand of the present study area with those in other areas along the Egyptian coasts (unit: Bq/kg).

Area	$e^{238}U$	$e^{232}Th$	$e^{226}Ra$	^{40}K	Reference
This study	20.501	18.216	36.853	469.85	
Industrial area of Port-Said	5.208	0.0525	-	3.756	Attia *et al*. (2015)
Port Said beach, Mediterranean Sea	12.37	6.16		223.30	Aziz *et al.* (2020)
Arish, Mediterranean Sea	-	7	8	197	Seddeek *et al.* (2005)
Delta, Mediterranean Sea	-	10	22	180	Ibrahim *et al*. (1993)
Baltim, Mediterranean Sea	-	198	132	236	Hilai. and Borai (2018)
Rosetta, Mediterranean Sea	-	53	56	120	El-Bahi *et al.* (2005)
Rosetta, Mediterranean Sea	42.76	38.71		168.12	Nada *et al*. (2012)
Rosetta, Mediterranean Sea	111.24-24.5	140.38-21.7	-	474.68-36.3	Abel-Rahman and El-Mongy (2017)
Coastal Red Sea of Egypt	22.7	11.6	21.1	930	Harb (2008)

Table 6: Comparison of radioactivity in the beach sand of the present study area with those in worldwide other areas (unit: Bq/kg).

Location	^{283}U	^{40}K	^{232}Th	^{226}Ra	Reference
The present study	20.501	18.216	36.853	469.85	
Abu Al Khasib, Arabian Gulf, Iraq	43.56	321.76	19.39	58.44	Mohammed and Ahmed (2017)
Coastline of Guangxi Province, China	11.9	39.6	9.6	6.9	Liu and Lin (2018)
Coast of Xiamen Island, China	ND	401.0	11.3	14.1	Huang *et al.* (2015)
Black sand in of Langkawi Island, Malaysia	ND	103	718	1478	Khandaker *et al.* (2018)
beach sand, coastal regions of Ramsar, Iran	ND	337.5	17.9	19.2	Tari *et al.* (2013)
Kirklareli, west coast of the Black Sea, Turkey	28±13	667±282	40±18	37±17	Taskin *et al*. (2009)
Beach sand Ilha Grande, Southeastern Brazil	ND	412	48	39	Freitas, and Alencar (2004)
Beach Sands from Rizhao Bathing Beach, China	ND	1079	15	12	Lu and Zhang 2008
Hungary	ND	302	28	28	UNSCEAR 2000

Conclusions

Radiological risk of the study area can be negligible because, values of radioactivity are less than the unity recommended by the International Atomic Energy Agency (IAEA, 1989) except the concentration of ^{40} K is higher than the acceptable limit. New Mansoura soil has aggressive behavior from intrusion of seawater and raises level in ground water surface.

References

ASTM, 2004. Standard test method for direct shear test of soils under consolidated drained conditions. Annual book of ASTM standards. D 3080, Sect. 4, Vol. 04.08. Philadelphia, Pa.

ASTM D-2216, Standard Test Method for Laboratory Determination of Water Content of Soil.

ASTM, D., 2011. Standard test method for standard penetration test (SPT) and split-barrel sampling of soils. ASTM Standard Test Method, 1586, 1-9.

ASTM D1586-18, Standard Test Method for Standard Penetration Test (SPT) and Split-Barrel Sampling of Soils

ASTM D5777-18, Standard Guide for Using the Seismic Refraction Method for Subsurface Investigation

ASTM D2216-19, Standard Test Methods for Laboratory Determination of Water (Moisture) Content of Soil and Rock by Mass

ASTM D6913-17, Standard Test Methods for Particle-Size Distribution (Gradation) of Soils Using Sieve Analysis

ASTM D3080-11, Standard Test Method for Direct Shear Test of Soils Under Consolidated Drained Conditions

ASTM D4254-16, Standard Test Methods for Minimum Index Density and Unit Weight of Soils and Calculation of Relative Density

ASTM D 854 – 02, Standard Test Methods for Specific Gravity of Soil Solids by Water Pycnometer

ASTM D2434 – 19, Standard Test Method for Permeability of Granular Soils (Constant Head)

ASTM D3042-17, Standard Test Method for Insoluble Residue in Carbonate Aggregates

Attia, T.E., E.H. Shendi and M.A. Shehata, 2015. Assessment of natural and artificial radioactivity levels and radiation hazards and their relation to heavy metals in the industrial area of Port Said city, Egypt. Environ Sci Pollut Res Int., 22(4):3082-97. doi: 10.1007/s11356-014-3453-z.

Aziz, A., T. Attia, and M. Hanafi, 2020. Radiological Impact and Environmental Monitoring of Gamma Radiations Along the Public Beach of Port Said, Egypt. Pure Appl. Geophys. 177, 2871–2876. https://doi.org/10.1007/s00024-019-02398-8

Belivermis, M., N. Kiliç, Y. Cotuk and S. Topcuoğlu, 2010. The effects of physicochemical properties on gamma emitting natural radionuclide levels in the soil profile of Istanbul. Environ Monit Assess., 163(1-4):15-26. doi: 10.1007/s10661-009-0812-1.

Beretka, J. and PJ. Matthew, 1985. Natural radioactivity of Australian building materials, industrial wastes and by-products. Health Phys., 48(1):87-95. doi: 10.1097/00004032-198501000-00007.

BS, 1377-3:2018: Methods of test for soils for civil engineering purposes - Chemical and electro-chemical testing

Conoco, 1987. Geologic Map of Egypt. Egyptian General Authority for Petroleum (UNESCO Joint Map Project), 20 Sheets, Scale 1:500 000. Cairo.

Das, B. M., 2010. Principle of Geotechnical engineering, Cengage Learning, Seven Edition, 683 P.

Das, B. M. 2011. Principles of Foundation Engineering, Global Engineering: Christopher M. Shortt, Seventh Edition, 815 P.

El-Bahi, S.M., N.W. El-Dine, F. Ahmed, A. Sroor and M.M. Abdl Salaam, 2005. Natural radioactivity levels for selected kinds of Egyptian sand. Isotopes Environ Health Stud., Jun;41(2):161-8. doi: 10.1080/10256010500054019.

El-Taher, A., S. Makhluf, A. Nossair, A.S. Abdel Halim, 2009. Assessment of natural radioactivity levels and radiation hazards due to cement industry. Applied Radiation and Isotopes, 68(1):169-174. https://doi.org/10.1016/j.apradiso.2009.09.001.

Faheem, M., S.A. Mujahid, Matiullah, 2008. Assessment of radiological hazards due to the natural radioactivity in soil and building material samples collected from six districts of the Punjab province-Pakistan. Radiation Measurements, 43(8):1443-1447. https://doi.org/10.1016/j.radmeas.2008.02.014.

Gelany, A.F.Y., M. A. Zeid, M.S. Abd El-Sadek and A. M. Mansour, 2019: Evaluation of the Expansive Esna Shale and Its Role in the Deterioration of Heritage Buildings at West Bank of Luxor. Journal of Geoscience and Environment Protection, 7(8):24-37.

Harb, S., 2008. Natural radioactivity and external gamma radiation exposure at the coastal Red Sea in Egypt, Radiation Protection Dosimetry, 130(3): 376–384, https://doi.org/10.1093/rpd/ncn064

Hilal, M.A. and E.H. Borai, 2018. Hazardous parameters associated with natural radioactivity exposure from black sand. Regul Toxicol Pharmacol., 92:245-250. doi:10.1016/j.yrtph.2017.12.014.

IAEA, 1989: International Atomic Energy Agency, measurement of radionuclides in food and the Environment. A Guidebook on Technical Report series No 295 IAEA, Vienna.

Ibrahiem, N.M., A.H. Abd el Ghani, S.M. Shawky, E.M. Ashraf and M.A. Farouk, 1993. Measurement of radioactivity levels in soil in the Nile Delta and middle Egypt. Health Phys., 64(6):620-7. doi: 10.1097/00004032-199306000-00007..

ICRP, 1990. Recommendations of the International Commission on Radiological Protection, 21(1–3), publication 60.

Lee, S. K., H.Wagiran, A.T. Ramli, N. H. Apriantoro and A. K. Wood, 2009. Radiological monitoring: terrestrial natural radionuclides in Kinta District, Perak, Malaysia, Journal of Environmental Radioactivity, 100(5), 368-37.4. https://doi.org/10.1016/j.jenvrad.2009.01.001.

Mamont-Ciesla, K., B. Gwiazdowski, M. Biernacka and A. Zak, 1982. Radioactivity of building materials in Poland (pp. p. 551–557.). John Wiley and Sons, Inc.

Ministry of Transport Japan, 1999: Design standard for port and harbor facilities and commentaries, Japan Port and Harbor Association, 438p.

NCRP, 1994. Exposure of the population in the United States and Canada from natural background radiation. NCRP Report No: 94. Bethesda, Maryland: NCRPM

Oktay, B., Ş. Karatepe and M. Doğru, 2010. Assessments of natural radioactivity and radiological hazards in construction materials used in Elazig, Turkey, Radiation Measurements, 46(1)153-158. https://doi.org/10.1016/j.radmeas.2010.08.010.

Örgün, Y., N. Altınsoy, S.Y. Şahin, Y. Güngör, A.H. Gültekin, G. Karahan, Z. Karacık, Natural and anthropogenic radionuclides in rocks and beach sands from Ezine region (Çanakkale), Western Anatolia, Turkey, Applied Radiation and Isotopes, 65(6):739-747. https://doi.org/10.1016/j.apradiso.2006.06.011.

Robertson, P. K. and C. E. Fear, 1997. Cyclic liquefaction and its evaluation based on the SPT and CPT In. Youd, T. Leslie, ed; Idriss, Izzat M., ed. Proceeding of the NCEER workshop on evaluation of liquefaction resistance of soils. Buffalo, N.Y, U.S. National Center for Earthquake Engineering Research (NCEER), Dec. 1997. p.41-87.

Seddeek, M.K., H.M. Badran, T. Sharshar and T.Elnimr, 2005. Characteristics, spatial distribution and vertical profile of gamma-ray emitting radionuclides in the coastal environment of North Sinai. J Environ Radioact.,84(1):21-50. doi: 10.1016/j.jenvrad.2005.03.005.

Seed, H. B. and I. M. Idriss, 1971: Simplified Procedure for Evaluating Liquefaction Potential. Journal of the Soil Mechanics and Foundations Division, ASCE, 107(SM9):1249-1274.

Seed, B., K. Tokimatsu, L. Harder and R.M. Chung, 1985: Influence of SPT procedures in soil liquefaction resistance evaluations, Journal of geotechnical engineering, 111(12): 1425-1445.

Shousha, H.A., M.R. Atta, A.A. Bakhit, H.M. Diab, A.A. El Hagg, and S. Dahy, 2019. Natural radioactivity assessment and the associated radiological hazards for beach sand, Baltim area, Egypt. Al-Azhar Bulletin of Science, 30(1-B), 37-47.

Shuaibu, H.K., M.U. Khandaker, T. Alrefae and D.A. Bradley, 2017. Assessment of natural radioactivity and gamma-ray dose in monazite rich black Sand Beach of Penang Island, Malaysia. Mar Pollut Bull.,15;119(1):423-428. doi: 10.1016/j.marpolbul.2017.03.026.

Taskin, H., M. Karavus, P. Ay, A. Topuzoglu, S. Hidiroglu and G. Karahan, 2009. Radionuclide concentrations in soil and lifetime cancer risk due to gamma radioactivity in Kirklareli, Turkey. J Environ Radioact., 100(1):49-53. doi: 10.1016/j.jenvrad.2008.10.012.

UNSCEAR, United Nations Scientific Committee on the Effects of Atomic Radiation, 1988. Sources, effects and risks of ionizing radiation. Report to the General Assembly, with annexes. United Nations, New York.

UNSCEAR, United Nations Scientific Committee on the Effects of Atomic Radiation, 2000. Sources and effects of ionizing radiation. United Nations Scientific Committee on the effect of atomic radiation. Report to the General Assembly, with Scientific Annexes. United Nations, New York.

Youd, T. L., I. M. Idriss, R.D. Andrus, I. Arango, G. Castro, J. T. Christian, R. Dobry, W.L. Finn, L. F. Harder and M. E. Hynes, 2003. Liquefaction Resistance of Soils: Summary Report from the 1996 NCEER and 1998 NCEER/NSF Workshops on Evaluation of Liquefaction Resistance of Soils" "Journal of Geotechnical Geoenvironmental Engineering, 129(3):284-286. https://doi.org/10.1061/(ASCE)1090-0241(2001)127:10(817)